

Investigation of density limit and MARFE by Polaris on J-TEXT tokamak

P. Shi¹, G. Zhuang², Z.P. Chen¹, the J-TEXT team

¹Huazhong University of Science and Technology, Wuhan Hubei, 430074, China

²University of Science and Technology of China, Hefei, 230026, China

Abstract

Multifaceted asymmetric radiation as well as strong poloidal asymmetry of the electron density from the edge, dubbed as “MARFE”, has been observed in high electron density Ohmically heated plasmas on J-TEXT tokamak. Equilibrium reconstruction based on the measured data from the 17-channel FIR polarimeter-interferometer indicates that an asymmetric plasma current density distribution forms at the edge region and the plasma current shrinkage locates at the MARFE affected region. Furthermore, associated with the localized plasma current shrinkage, a locked mode MHD activity is excited, which then terminate the discharge with a major disruption. Localized plasma current shrinkage at the MARFE region is considered to be the direct cause for the density limit disruptions, and the proposed interpretation is consistent with the experimental observations.

1. Introduction

The thermonuclear power in a tokamak reactor is proportional to the square of electron density ($\sim n_e^2$) demands that the future tokamak reactors must operate at high density safely. However, the existence of density limit disruption [1,2] can be an important obstacle to that goal. Recently, the experiment for investigation of density limit disruption has been carried out on J-TEXT tokamak. The phenomenon of multifaceted asymmetric radiation from the edge (dubbed a “MARFE”) during density limit discharge has been identified firstly on J-TEXT by several diagnostics. During the MARFE evolution, strong poloidal asymmetry of electron density and line radiation at edge has been observed. Besides, it is found that the plasma current distribution also shows asymmetric behavior at edge, by analyzing the data from FIR polarimeter-interferometer (POLARIS). Based on the experimental observations, a new mechanism is proposed to explain the density limit disruptions associated with MARFEs.

2. Experiment

The experimental observations of high-density discharges on J-TEXT confirm that these discharges are frequently disrupted as the plasma density approaches an upper limit and they have almost identical performance. A typical high-density disruption discharge (shot #1038116) is shown in Fig. 1. The discharge is terminated at $t = 0.41$ s and the maximum central line-averaged density is $5.6 \times 10^{19} \text{m}^{-3} = 0.67 n_G$, where n_G is the Greenwald density [3]. During the interval of $0.2 \text{ s} < t < 0.4 \text{ s}$, the central (at $r = 0$ cm) line-averaged electron density $n_e(0)$ keeps increasing (Fig. 1(d)) and n_e at $r = -24$ cm (very edge of HFS) suddenly surges upward at about $t = 0.33$ s while it changes little or even drops at $r = 24$ cm (very edge of

LFS) as shown in (Fig. 1(e)). At the same time of HFS edge density surging upward, the C_{III} line emission at HFS edge also soars upward, as Fig. 1(f) shows. Fig. 1 indicates that an asymmetry of density and C_{III} line emission profiles occurs between the very edge of LFS and HFS. The plasma horizontal displacement is stable after 0.3 s, as shown in Fig. 1(d). So the effect of plasma displacement on the edge density variation can be excluded. Additionally, the plasma horizontal position can be manifested by the Faraday rotation angle (α) near the magnetic axis. As showed in Fig. 1(j), the α at $r=3cm$ almost remains constant near zero during the edge density asymmetry increasing, indicates that the global position of plasma column changes little. Therefore, it can be concluded that the electron density asymmetry on the same magnetic surface occurs at edge. In addition, the visible CCD camera records a bright blob at the edge of HFS after that asymmetric plasma behaviors occur, as shown in Fig. 1(k). It is observed that a bright blob appears and locates outside of the plasma at $t = 0.30 s$, however, there is no asymmetry (between the LFS and HFS edge region) in the radial profiles of the electron density and C_{III} emission, as shown in Fig. 1(e) and 1(f). As time evolves, the blob gets brighter and moves into the edge region of the plasma for $t = 0.34 s$, and the asymmetry in the profiles of n_e , $I_{C_{III}}$ and B_θ are enhanced. Afterwards, the bright blob stays inside the plasma edge region for a few tens milliseconds, then it gradually rotates poloidally at $t = 0.39 s$ and the discharge is terminated by a disruption at $t = 0.41 s$. The diagnostic signals above indicate that a poloidally local region with high density and strong line emission forms at HFS edge after plasma density exceeds a threshold before density limit disruption. All the characteristics of this phenomenon are referenced to the MARFE, which always occurs in high density tokamak plasma.

In Fig. 1, the Faraday rotation angle measured by POLARIS is proportional to the product of electron density and parallel magnetic field, $\alpha \sim \int n_e B_{\parallel} dz$. Therefore, the ratio (α/n_e) between Faraday rotation angle and electron density is strongly dependent on B_{\parallel} . To some degree, the evolution of α/n_e reflects the variation of B_{\parallel} . The radial distribution of α/n_e for discharge in Fig. 1 is plotted in Fig. 2(d). Additionally, Fig. 2 also plots the radial distributions of line-averaged electron density (Fig. 2(a)) measured by the POLARIS, radiation power (Fig. 2(b)) by the AXUV measurement, intensity of C_{III} line emission (Fig. 2(c)). After MARFE onsets (0.34 s and 0.39 s), the radial distributions of line-averaged electron density and C_{III} line emission appear significantly asymmetry at the edge, being consistent with the data in Fig. 1. Besides, the asymmetric distribution is also observed on α/n_e , which decreases greatly at HFS edge after MARFE onset, meanwhile, α/n_e at other positions almost remains constant during the plasma density increasing. The value of α/n_e at $r = -24 cm$ decreases by more than 60% from the time of MARFE onset to disruption. According to the occurring time and location, the decrease of α/n_e at HFS edge is inferred to be result of MARFE, just similar to the increase of density and line radiation.

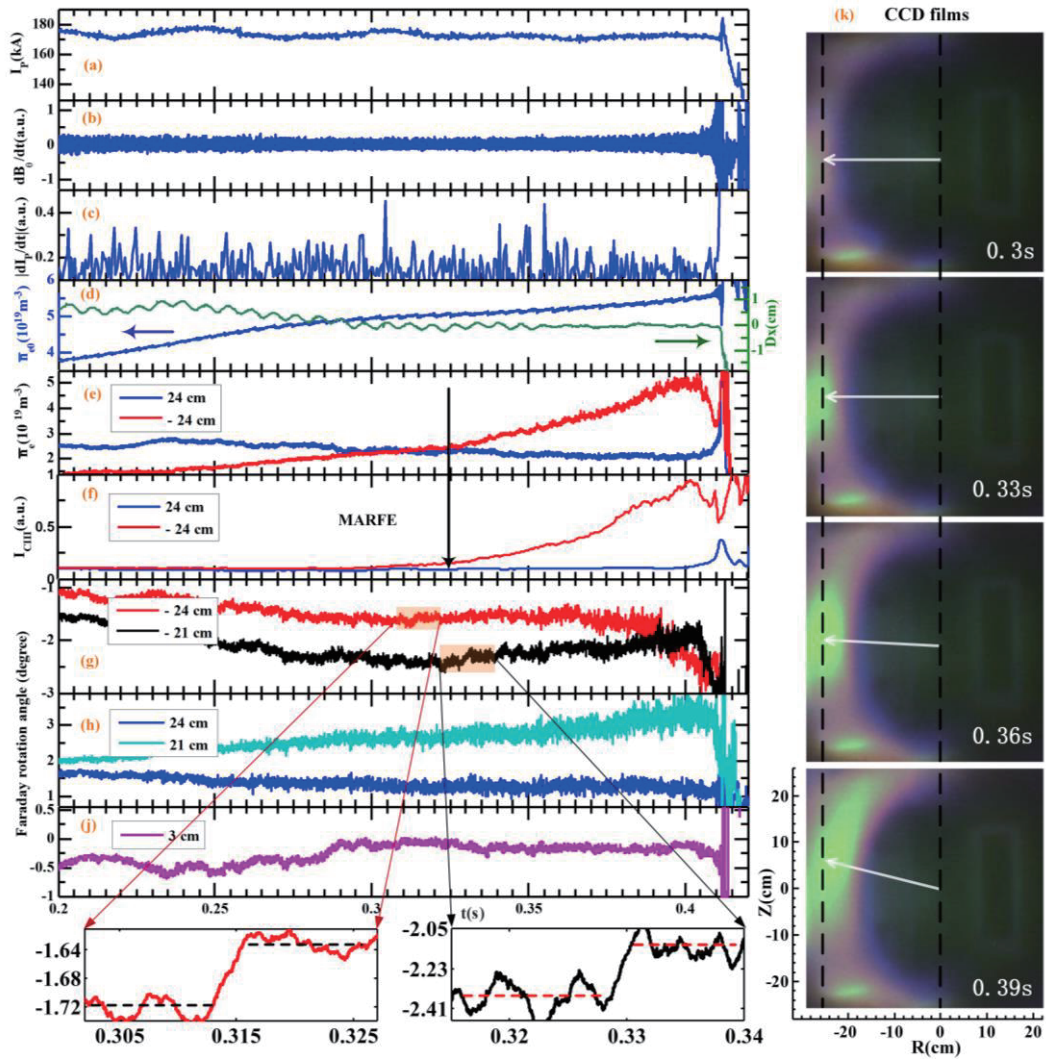


Fig.1 A typical density limit disruption discharge. (a)The total plasma current, (b) the edge magnetic coil signal, (c) dI_p/dt from a magnetic probe, (d) central line-averaged density measured by FIR polarimeter-interferometer and the plasma horizontal displacement, (e) line-averaged density at $r=\pm 24$ cm, (f) CIII line emission at $r=\pm 24$ cm, the 2-channel line-integral Faraday angle at the edge of (g) HFS and (h) LFS, (i) the line-integral Faraday angle at $r=3$ cm, (k) CCD camera records.

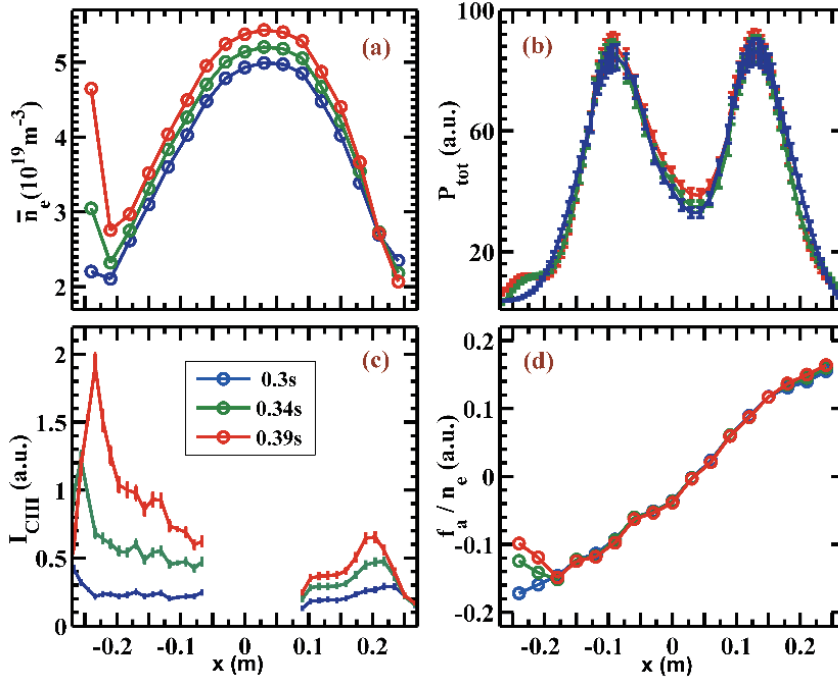


Fig.2 Time evolution of radial distributions of (a) line-averaged electron density measured by POLARIS, and (b) radiation power profiles measured by AXUV, and (c) CIII line radiation intensity obtained by PDA array, and (d) ratio of line-integral Faraday rotation angle to electron density from the POLARIS.

3. Discussion

In order to understand the POLARIS data, the whole plasma region is divided into three regions, as shown in Fig. 3(a), where Region A is the innermost region with symmetric distribution of plasma current, Region B marks the region where the magnetic field lines distort at the edge of MARFE area (similar to a ‘limiter’), and Region C is the MARFE area where the plasma current is approximated by zero. Corresponding to the 2-D distribution of plasma current density and electron density, the radial profiles of current density and electron density at midplane ($Z=0$) are shown in Fig. 3(c) and 3(d), together with the symmetric results from ERP, which removed the four channels at HFS edge. Furthermore, the line-integral Faraday rotation angle and electron density are obtained and shown together with the measured results and ERP results in Fig. 3(e) and 3(f), respectively. It is observed from Fig. 3(e) and 3(f) that the calculated Faraday rotation angle and electron density from the reconstructed current and density distributions are in agreement with the POLARIS measurements, indicating that localized plasma current shrinkage at the MARFE region is pronounced and reasonable.

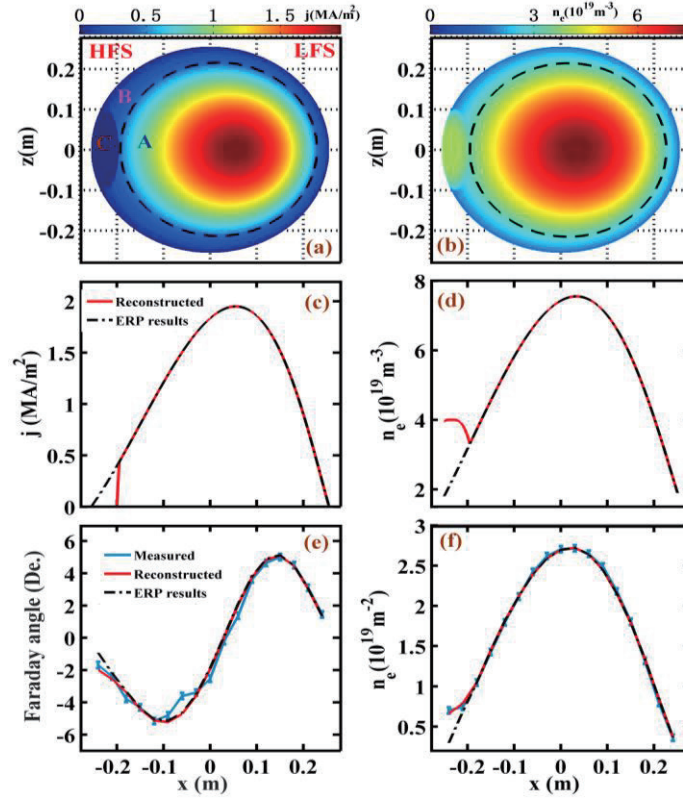


Fig.3 (a) The constructed plasma current distribution, (b) the constructed electron density distribution, (c) the plasma current profile at the midplane from that plasma current distribution and ERP results, (d) the electron density profile at the midplane from that electron density distribution and ERP results, (e) the line-integral Faraday rotation angle, and (f) line-integral electron density from the reconstructed plasma current and electron density distributions, ERP results and POLARIS measurements.

Since the localized plasma current shrinks in the MARFE region, the symmetry of confined magnetic field structure is broken, the radial magnetic field is no longer zero. The distribution of radial magnetic field is obtained by taking the non-zero current density in Region B into account as shown in figure 4(a), and the radial magnetic field along $q = 2$ surface is also shown in Fig. 4(b). It is found that the radial magnetic field reach $\sim 100G$ at the $q = 2$ surface, and it would have the similar effect as error magnetic field. When the asymmetry expands into the inner region of plasma, the influence of the MARFE on the edge region of HFS gets larger, and the magnitude of the radial magnetic field becomes considerably larger and much closer to the $q = 2$ rational surface. At last the strong enough radial magnetic field may trigger locked mode and a major disruption happens. The Fig. 4 (c) plots the 2-D distribution of poloidal magnetic field difference (ΔB_θ) between with and without current shrinkage. It shows that the current shrinkage caused by MARFE has strong influence on the B_θ nearby the HFS edge, while it has little effect on the B_θ at LFS. The Fig. 4 (d) plots the ΔB_θ distribution at $|r|=0.312 m$. It shows that the B_θ at 180° decreases $\sim 50 G$ after the current shrinkage occurring. It is reasonable comparing to the experimental result. The results indicate that the localized plasma current shrinkage may be the cause for density limit disruption.

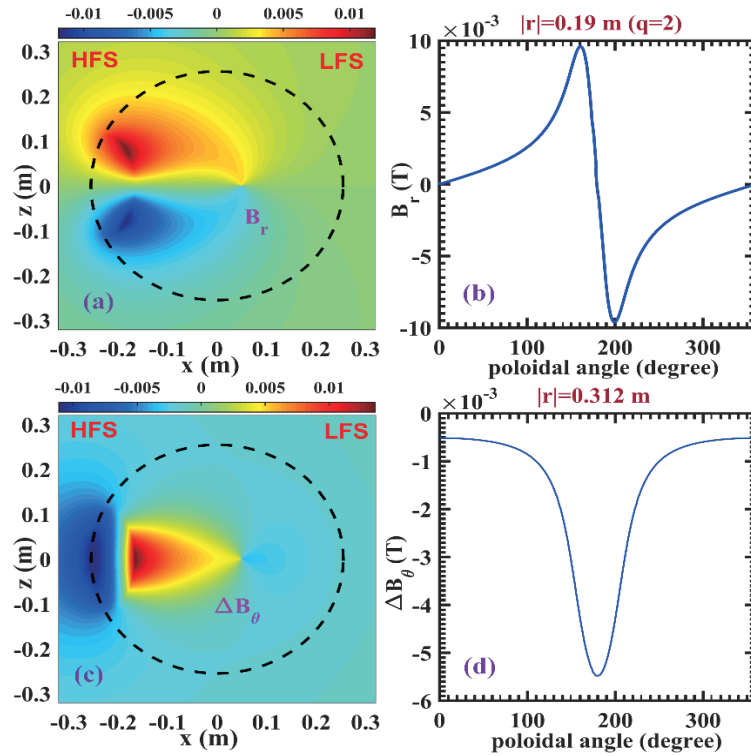


Fig.4 (a) the radial magnetic profile for entire section; (b) the radial magnetic profile at $q=2$ surface; (c) the profile of poloidal magnetic difference (ΔB_θ) between with and without current shrinkage; (d) profile of ΔB_θ at $|r|=0.312$ m (the Mirnov coils position). The black dash lines indicate the LCFS surface ($|r|=25.5$ cm).

4. Summary

The high density Ohmically heated plasma characterized by MARFEs has been observed on the J-TEXT tokamak, and those discharges always end by a major disruption. The MARFEs on J-TEXT are mainly characterized by a poloidally localized region with high density and strong line emission occurring at HFS edge, and a ‘bright blob’ at HFS edge getting into the plasma. At the time of MARFE onset, a sudden drop on Faraday rotation angle at HFS edge is observed, infers a sudden change of plasma current density at HFS edge. By further analyzing the data from 17-channel POLARIS, the poloidal asymmetry on poloidal magnetic field during MARFEs has been found for the first time. Based on the measured electron density and Faraday rotation angle data, asymmetric density profiles and plasma current density distributions are reconstructed. The constructed plasma current density distribution indicates that the plasma current shrinks in the MARFE region. Such localized plasma current drop would produce a radial magnetic field of ~ 100 G around the $q = 2$ surface, which may be sufficient to trigger the 2/1 locked mode and cause the major disruption. The results presented in this letter offer a possible interpretation for the mechanism of MARFE and density limit disruptions.

Acknowledgements

This work was partly supported by the JSPS-NRF-NSFC A3 Foresight Program in the field of Plasma Physics (NSFC: No.11261140328, NRF: No.2012K2A2A6000443).

Reference:

- [1] Murakami M. Callen J. D. and Berry L. A. 1976 Nucl. Fusion 16 347
- [2] Greenwald M. et al 1988 Nucl. Fusion 28 2199
- [3] Greenwald M. 2002 Plasma Phys. Control. Fusion 44 R27